# Neural network potential for CrCoNi system (Version 2)

Jun-Ping Du[a,*], Shigenobu Ogata[a,*]

[a]*Department of Mechanical Science and Bioengineering, Osaka University, Osaka 560-8531, Japan.*

## 1. Architecture of NNP

We adopted the high-dimensional neural network potential (NNP) developed by Behler and Parrinello [1] to construct the NNP for CrCoNi medium entropy alloy. The energy of system in the NNP is expressed as

$$E_{tot} = \sum E_n, \tag{1}$$

where $E_n$ is the atomic energy. The atomic energy is calculated as

$$E_n = f_1^3\left\{b_1^3 + \sum_k a_{k1}^{23} * f_k^2\left[b_k^2 + \sum_j a_{jk}^{12} * f_j^1(b_j^1 + \sum_i a_{ij}^{01} * G_i)\right]\right\} \tag{2}$$

where $f_1^3(x) = x$, $f_k^2(x) = \ln(1 + \mathrm{e}^x)$, and $f_j^1(x) = \ln(1 + \mathrm{e}^x)$ are the activation functions, $b_1^3$, $b_k^2$, $b_j^1$, $a_{k1}^{23}$, $a_{jk}^{12}$, and $a_{ij}^{01}$ are the weight parameters of NNP, $G_i$ is the symmetry functions characterized the local chemical environments of the atom. The following 3 types of symmetry functions were adopted for atom $i$ and its all neighbors $j$ and $k$,

$$G_i^2 = \sum_j \mathrm{e}^{-\eta R_{ij}^2} f_c(R_{ij}), \tag{3}$$

$$G_i^3 = 2^{1-\xi} \sum_{j\neq i} \sum_{k\neq i,j} \left[(1 + \lambda\cos\theta_{ijk})^{\xi} \mathrm{e}^{-\eta(R_{ij}^2 + R_{ik}^2 + R_{jk}^2)} f_c(R_{ij}) f_c(R_{ik}) f_c(R_{jk})\right], \tag{4}$$

and

$$G_i^9 = 2^{1-\xi} \sum_{j\neq i} \sum_{k\neq i,j} \left[(1 + \lambda\cos\theta_{ijk})^{\xi} \mathrm{e}^{-\eta(R_{ij}^2 + R_{ik}^2)} f_c(R_{ij}) f_c(R_{ik})\right], \tag{5}$$

where $\eta$, $\xi$, $\lambda$ are pre-defined parameters before training the NNP. The $f_c(R_{ij})$ is a cutoff function defined as

$$f_c(R_{ij}) = \begin{cases} \tanh^3(1 - R_{ij}/R_c), & R_{ij} \leq R_c \\ 0, & R_{ij} > R_c \end{cases} \tag{6}$$

*Email: jpdu@tsme.me.es.osaka-u.ac.jp (J.P.D.), ogata@me.es.osaka-u.ac.jp (S.O.)

and the cutoff distance $R_c = 6$ Å. For each element, we used 171 symmetry functions in the input layer. Between the input layer and the output layer, there are 2 hidden layers and each hidden layer contains 15 nodes.

## 2. DFT training dataset

A. To sample the inequivalent configurations systematically, we used the *mmaps* code of the ATAT package [2] to generate a set of inequivalent atomic configurations with up to 7 atoms and 3 types of elements in a primitive cell. The atoms arrangements were set in FCC, BCC, and HCP structures in the primitive cells, respectively. The possible composition of the ternary alloys in the primitive cells ($Cr_xCo_yNi_z$) is constrained by $0 \leq x \leq 1$, $0 \leq y \leq 1$, $0 \leq z \leq 1$, and $x + y + z = 1$, so that our NNP potential can be used not only in equiatomic HEA, but also in the monoatomic or binary atomic solid solution, e.g. in the condition of phase separation of HEA. These primitive cells constructed by *mmaps* were relaxed with respects to cell volume, shape, and atomic positions using VASP [3–5]. To describe the elastic properties of HEA, the relaxed primitive cell consisting of $1 \sim 6$ atoms were applied to three types of deformation on the cell lattice, that is $(\delta, \delta, \delta, 0, 0, 0)$, $(1+\delta', 1-\delta', 0, 0, 0, 0)$, and $(0, 0, 0, \delta', 0, 0)$, where $0.9 \leq \delta \leq 1.15$ and $0 \leq \delta' \leq 0.05$ with an interval of 0.01. The static calculation results of the deformed primitive cells were included in the DFT datasets. The vacancy is one of the elementary lattice defects, which is related to the diffusion of metal atoms in the HEAs and the formation of SRO. Thus, we also prepared the primitive cells of FCC–CrCoNi with vacancy using *mmaps*, where vacancy concentration is equal or less than 0.25 and the models were relaxed with respects to cell volume, shape, and atom positions using VASP.

B. To include the atomic configurations of vacancy diffusion, 24 diffusion pathways in an equiatomic $(3 \times 3 \times 3)a_0$ FCC–CrCoNi model and each pathway consisting of 5 images obtained by NEB calculations [6, 7] with VASP are included in the DFT datasets.

C. In order to include the information of SRO in the training dataset, we adopted an ordered equiatomic $(3\times3\times3)a_0$ FCC–CrCoNi model, where $a_0 = 3.52$ Å and Cr, Co, and Ni, respectively, occupied one $(3\times3\times1)a_0$ regions. Then, we performed 1,000 times of swapping of two atoms with different types of elements successively. After every swapping, the static energies were calculated using VASP and also included in the DFT datasets.

D. We also performed first-principles molecular dynamic (FPMD) simulations under fixed volume and temperature to sample the configurational space deviated from their equilibrium positions. Based on a $(2 \times 2 \times 2)a_0$ FCC supercell with 31 atom and one vacancy, where $a_0 = 3.5$ Å, we generated 21 supercell models by randomly setting the type of the atoms as Co, Cr or Ni with equal probability. The temperature of the FPMD simulations ranges from 300 K to 1500 K with an interval of 300 K.

Table 1: The number of supercell model ($N_{supercell}$) and the corresponding total number of atoms ($N_{atom}$) in the DFT datasets used to construct the NNP for the MEA CrCoNi. The dataset labeled by an asterisk and a dagger were fully and partly generated in this work, respectively. The reminding dataset were generated in Ref. [10].

| DFT dataset | $N_{\text{supercell}}$ | $N_{\text{atom}}$ |
|---|---|---|
| A | 72861 | 460100 |
| B | 1913 | 204691 |
| C | 1001 | 108108 |
| D | 49086 | 1521666 |
| E$^{\dagger}$ | 5771 | 623268 |
| F | 9034 | 830090 |
| G$^{*}$ | 3059 | 236148 |
| H | 16323 | 205912 |
| I | 2803 | 5606 |

E. Accompanying with the crystalline structure, the models of equiatomic HEA with liquid state are also included in the DFT datasets. Ten models with 108 atoms randomly located within in $(3 \times 3 \times 3)a_0$ supercells were designed. Then, the $a_0$ were set as 3.6 Å, 3.8 Å, and 4.0 Å, respectively, and the FPMD simulations were performed at the temperature of 2000 K to model the liquid state of the HEA at different density.

F. The equiatomic HEA with (100), (110), (111), and (112) surfaces were designed using slab models and FPMD simulation were performed at 300 K and 600 K.

G. The FCC–Ni and BCC–Cr with (100), (110), (111), and (112) surfaces, and HCP–Co with (0001), (1000), and (1120) surfaces were designed using slab models and FPMD simulation were performed at 300 K.

H. The cluster models contain 3, 4, 5, and 55 atoms. The FPMD simulation were performed at 300 K for the models.

I. The equation of state (EOS) of 6 kinds of dimers (Cr–Cr, Cr–Co, Cr–Ni, Co–Co, Co–Ni, and Ni–Ni) were fitted using the FPMD simulations at 300 K with the universal EOS [8], $E(r_{ij}) = E_0(1 + \frac{r_{ij}-r_e}{a}) * e^{-\frac{r-r_e}{a}} + E_{i,a} + E_{j,a}$, where $E_0$, $r_e$, $a$, $E_{i,a}$, and $E_{j,a}$ are fitting parameters. $E_{i,a}$ and $E_{j,a}$ denote the atomic energies of the dimer from DFT calculations for atoms i and j, respectively. The training dataset related to the dimer were created from the universal EOS. The bond lengths of the dimers range from about $1 \sim 1.5$ Å to the cutoff distance.

The exchange correlation between electrons in the collinear-spin-polarized DFT calculations was treated with the generalized gradient approximation [9] in the PBE form and the energy cutoff was $1.3 \times E_{\max}$, where $E_{\max}$ is the largest value of the default maximum energy cutoff of the plane-wave basis of Cr, Co and Ni.

## 3. Construction of NNP

The total DFT dataset consists of 161,851 structures (4,195,589 atoms). The energies of the structures and the forces of all atoms were used to train the NNP with the n2p2 code [11]. In the n2p2 code, the DFT training dataset are divided into two part: training data and testing data. 90% of structures were randomly selected as the training data and the remanding data were used as the testing data. The comparison between the energies and the forces from the DFT and the NNP are shown in Fig. 1. The root of mean squared error of both the training data and the testing data are 17 meV/atom for the energies, and 0.13 eV/Å for the forces.

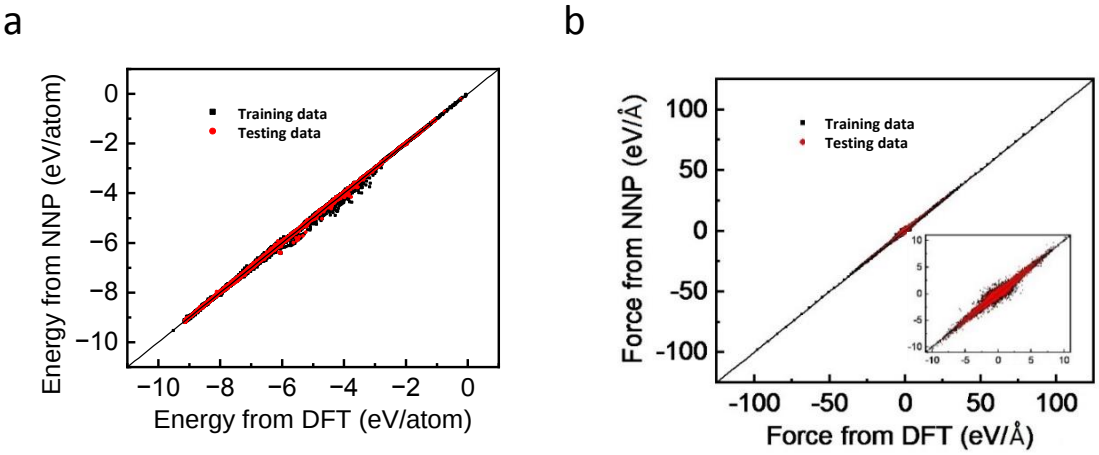


Figure 1: Energies and forces of training and testing data from the DFT calculations and the NNP. The solid lines indicate the points where the DFT results equals to the NNP results.

## References


[1] Jörg Behler and Michele Parrinello. Generalized neural-network representation of high-dimensional potential-energy surfaces. *Physical review letters*, 98(14):146401, 2007.

[2] Axel Van De Walle. Multicomponent multisublattice alloys, nonconfigurational entropy and other additions to the alloy theoretic automated toolkit. *Calphad*, 33(2):266–278, 2009.

[3] Georg Kresse and Jürgen Hafner. Ab initio molecular dynamics for liquid metals. *Physical Review B*, 47(1):558, 1993.

[4] Georg Kresse and Jürgen Hafner. Ab initio molecular-dynamics simulation of the liquid-metal–amorphous-semiconductor transition in germanium. *Physical Review B*, 49(20):14251, 1994.

[5] Georg Kresse and Jürgen Furthmüller. Efficient iterative schemes for ab initio total-energy calculations using a plane-wave basis set. *Physical review B*, 54(16):11169, 1996.

[6] Hannes Jónsson, Greg Mills, and Karsten W Jacobsen. Nudged elastic band method for finding minimum energy paths of transitions. 1998.

[7] Graeme Henkelman, Blas P Uberuaga, and Hannes Jónsson. A climbing image nudged elastic band method for finding saddle points and minimum energy paths. *The Journal of chemical physics*, 113(22):9901–9904, 2000.

[8] James H Rose, John R Smith, Francisco Guinea, and John Ferrante. Universal features of the equation of state of metals. *Physical Review B*, 29(6):2963, 1984.

[9] John P Perdew, Kieron Burke, and Matthias Ernzerhof. Generalized gradient approximation made simple. *Physical review letters*, 77(18):3865, 1996.

[10] Peijun Yu, Jun-Ping Du, Shuhei Shinzato, Fanshun Meng, and Shigenobu Ogata. Theory of history-dependent multi-layer generalized stacking fault energy-a modeling of the micro-substructure evolution kinetics in chemically ordered medium-entropy alloys. *Acta Materialia*, 224:117504, 2021.

[11] Andreas Singraber, Tobias Morawietz, Jörg Behler, and Christoph Dellago. Parallel multistream training of high-dimensional neural network potentials. *Journal of chemical theory and computation*, 15(5):3075–3092, 2019.